24th IMEKO TC4 International Symposium
22nd International Workshop on ADC and DAC Modelling and Testing
IMEKO TC-4 2020
Palermo, Italy, September 14-16, 2020

High capacitance simulation using mutual inductors

Stanislav Mašláň[1]

[1]*Czech metrology institute, Okružní 31, 638 00 Brno, smaslan@cmi.cz*

***Abstract* – This paper describes experimental high capacitance simulator based on a mutual inductance. The standard was designed for calibration of battery impedance analyzers (EIS). The designed standard is equipped by a DC bias voltage source designed to simulate typical lithium battery cell. The DC bias source was designed so it does not affect properties of simulated impedance by its own internal impedance. The whole standard was designed for a frequency range from fraction of hertz to at least 5 kHz and it can withstand peak measurement current up to 2.5 A.**

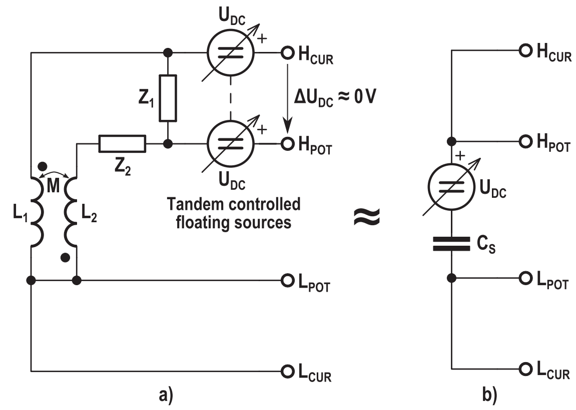

Fig. 1. Principle circuit diagram of capacitance simulator based on mutual inductor. a) Principle connection, b) equivalent circuit.

I. INTRODUCTION

Impedance spectroscopy (EIS) of batteries is one of the most common laboratory methods used to analyze state of charge (SoC) and state of health (SoH) parameters of batteries. Typical lithium cell internal impedance may vary from sub-milliohm values for large cells with capacity of tens of amper-hours up to tens of milliohms for e.g. regular 18650 cells. The characteristic features in the frequency spectrum, the semicircles in nyquist domain which are being used to evaluate SoC and SoH, lie typically in a frequency range from tens of millihertz up to few tens or hundreds of hertz. Traceability in this range of impedances and frequencies is not well established even in primary impedance laboratories of national metrology institutes (NMI) and even less in electrochemistry laboratories. The measurements performed in particular laboratories are often not repeatable and comparable. This situation was identified as a major problem by consortium of EMPIR [1] project "LiBforSecUse - Lithium Batteries for Second Life Applications" [2]. Thus one of the basic goals of this project is to improve metrology of low impedances down to very low frequencies. Several approaches for construction of reference standards were suggested: (i) Passive resistive standards based on coaxial current shunts; (ii) Analogue active simulators based on power amplifiers; (iii) Digital simulators derived from METAS concept [3]; (iv) Analogue capacitance simulator based on mutual inductances.

Passive standards (i) based on coaxial shunts provide excellent source of traceability from DC to at least hundreds of kilohertz. They can be manufactured easily down to order of milliohms and calibrated on ac-dc difference with uncertainties around 10 μΩ/Ω and phase angle of few microradians. Alternatively they can be made calculable [4]. The two port coaxial connection can be converted to four terminal pair (4TP) without significant mutual couplings using approach shown in [5]. However, these standards are almost purely resistive, whereas the actual impedance spectrum measurement covers full complex plane. Furthermore the DC bias should be somehow applied in order to simulate the cell.

Analogue active electronic simulators (ii) are based on the impedance multipliers using power operational amplifiers. These circuits allow to scale regular impedances in order of microfarads and kiloohms to order of farads. However, eventual introduction of DC bias to these circuits may result in variation of simulated impedance due to change of DC operating point of active components (limited common mode rejection, nonlinearity, etc.).

Digital simulators (iii) are based on measurement and phase locking to H_{POT} terminal potential of a RLC/EIS meter and injecting complex current proportional to the simulated impedance to the RLC meter's L_{CUR} terminal as shown in [3]. This method is very accurate and it can simulate any impedance in full complex plane, however it is not applicable to all RLC/EIS meters. When the meter does not produce continuous sine wave drive signal on its H_{CUR} terminal, it is very challenging to synchronize the simulator and to force the instrument to accept the simulated signals.

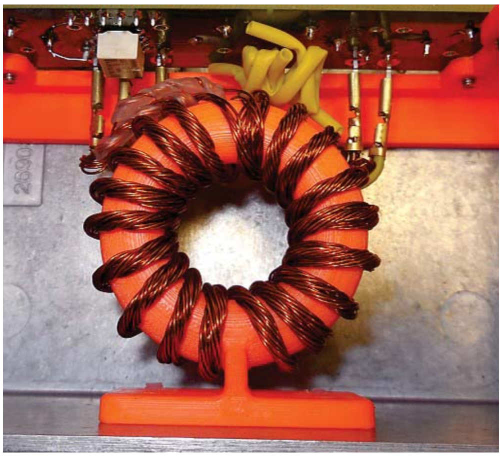

Fig. 2. Realization of prototype of mutual inductor on a 3D printed holder. Outer diameter is approx. 40 mm.

All above mentioned methods are used in scope of the new EMPIR project LiBforSecUse to build a set of experimental low impedance standards covering low impedances down to at least 1 mΩ. Following paper will describe yet another method based on the mutual inductors (iv). This method produces capacitive reactance with optional DC bias up to kilofarad order.

II. BASIC CONCEPT

The target impedance of the simulator is a capacitive reactance in a range from sub-milliohm up to tens of milliohms at frequencies around 1 Hz. That is roughly equal to capacitances from 10 F to 1 kF which obviously cannot be realized by the physical capacitors. Although there are supercapacitors reaching these values, they always exhibit strong DC bias and current dependencies and also temperature dependencies, so they are not directly usable as calibration standards. Therefore an experiment was carried out using a mutual inductor. If the polarity of the secondary coil of mutual inductor is inverted, it will appear to the impedance analyzer as a capacitive reactance approximately according formula:

$$C_\mathrm{S} \approx \frac{1}{\omega^2 \cdot M}, \tag{1}$$

where ω is angular frequency of measurement and M is mutual inductance between the coils. The impedance and its phase angle can be slightly trimmed by the optional network formed of impedances Z_1 and Z_2. Unpleasant feature of this concept is frequency dependence, so this standard is usable only at limited range of frequencies as the value of capacitance C_S is dependent on the inverse square of frequency. On the other hand it allows to realize capacitances up to order of kilofarads capable to withstand measurement currents in order of amperes with minimum temperature dependence and it can be also very linear.

III. DESIGN OF STANDARD

The mutual inductor itself is just part of the simulator. The more challenging part is simulation of the DC bias voltage. There are three ways of applying the bias voltage. The simplest is to place a floating source in series with the potential terminal $\mathrm{H_{POT}}$. In this case the source carries almost no current, so it is simple to design. In the simplest case it can even be a battery. However, some EIS meters may not stand the potential difference between their $\mathrm{H_{POT}}$ and $\mathrm{H_{CUR}}$ terminals. Alternative solution may be to place a DC source in series with the whole standard, however that would destroy its properties as internal impedance of the source would became part of the impedance. So a third way based on two floating tandem controlled sources was chosen as shown in Fig. 1. The source in series with the $\mathrm{H_{CUR}}$ terminal has to carry full measurement current, but its accuracy is not critical. The second floating source is connected in series with $\mathrm{H_{POT}}$ terminal. It carries almost no current so its internal impedance is not critical but it should be accurate, low noise and should have minimum capacitive coupling to the power supply. If both sources are set to identical DC voltage, the EIS meter will see roughly zero DC voltage drop between its $\mathrm{H_{POT}}$ and $\mathrm{H_{CUR}}$ terminals so its function should not be affected. Advantage of this solution is also the varying DC voltage does not affect the simulated impedance unlike fully electronic simulators based on power amplifiers that would be affected by common mode rejection and nonlinearities.

The mutual inductor itself was realized as a toroidal coil on a 3D printed holder as shown in fig. 2. This way most of the magnetic flux is contained inside the toroidal area. It is a method commonly used for a close field metrology grade inductance standards, such as IET 1482 or russian R5100 series. Therefore it is not excessively sensitive to nearby metallic objects and external magnetic fields and the induction to the metal case is also minimized, so the inductance is reasonably linear. The winding in the prototype is made of 20 twisted enamelled wires. Ten of them are connected in parallel to form a primary. The other ten wires are connected in series as a secondary winding with tap on the first wire section, so it is possible to switch two mutual inductances in ratio 10:1. The secondary coil also contains polarity switch, so it can inverse capacitive/inductive reactance theoretically without changing absolute reactance value.

The proof of concept prototype was built and its design was made available as open hardware project [6] for further development. The basic concept from Fig. 1 was extended to 4TP coaxial connection, so a true 4TP standard was realized. Block diagram of the analogue part of the standard is shown in Fig. 4. The potential coil L_2 is equiped by a "Range" relay that switches the taps. Polarity of the coil is switched by dual "Polarity" relay. Finally, for experimental purposes, the whole potential and current part of

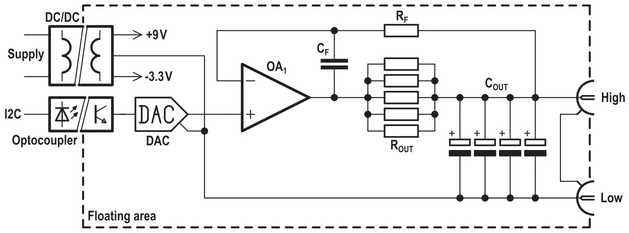

Fig. 3. Simplified connection of floating DC bias sources to be connected in series with H_{POT} and L_{POT} terminals of simulated impedance.

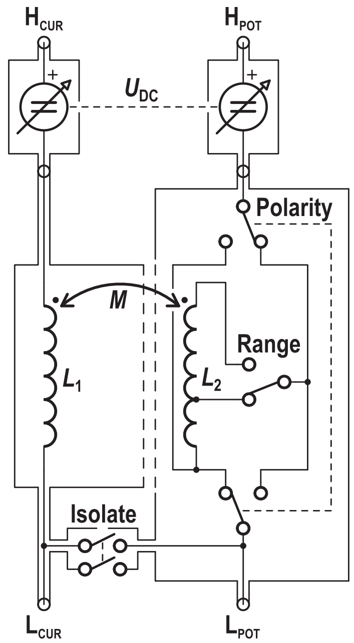

Fig. 4. Four terminal-pair connection of the simulated standard.

the standard can be split by the "Isolate" relay. This may be useful for some types of bridges and it has not strong effect to the standard value apart from the inevitable capacitive coupling in the mutual coil itself.

This strict separation of the potential and current grounds is critical feature when calibrating the RLC/EIS meters at low impedances, because it eliminates difference between four or five terminal (4T/5T) and 4TP impedance definition. The problem of 4TP impedance definition is illustrated in the Fig. 5. For 4T/5T measurement, the shield impedance $\hat{Z}_G$ is ignored and impedance is calculated simply:

$$\hat{Z}_{4T/5T} = \frac{\hat{U}_X}{\hat{I}_X} = \hat{Z}_X, \qquad (2)$$

where $\hat{U}_X$ is voltage drop between H_{POT} and L_{POT} live terminals, $\hat{I}_X$ current via the standard and $\hat{Z}_X$ is internal impedance of the standard. If the standard is made without separation of the potential and current grounds and the

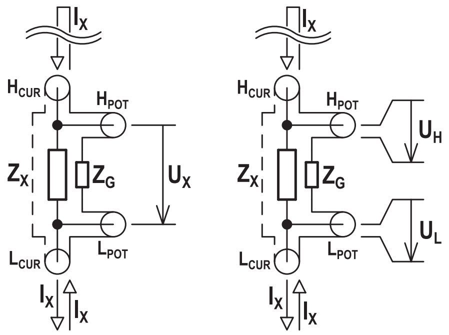

Fig. 5. Four terminal-pair (4TP) vs four- or five-terminal (4T/5T) definition of the impedance.

BNC ports are simply mounted inline in a metal sheet, there will be impedance $\hat{Z}_G$ between the H_{POT} and L_{POT} terminal grounds. Opposite current flows via this the shield and causes additional voltage drop. 4TP definition is given by formula:

$$\hat{Z}_{4TP} = \frac{\hat{U}_H - \hat{U}_L}{\hat{I}_X} = \hat{Z}_X + \hat{Z}_G, \qquad (3)$$

where $\hat{U}_H$ and $\hat{U}_L$ are port voltages measured at the standard. Therefore $\hat{Z}_G$ becomes part of the measured 4TP impedance. The problem is RLC/EIS meters often cannot measure properly potential difference between the grounds of H_{POT} and L_{POT} terminals below few kilohertz because it requires either differential input amplifiers at their H_{POT} and L_{POT} inputs or current equalization using coaxial chokes which are mostly present, but they are not effective at low frequencies. Some impedance standards have large effective ground impedance $\hat{Z}_G$ so it easily results in offsets in the measured value by up to some 500 μΩ which gradually disappears at higher frequencies when the current equalization takes place. This behaviour is obviously different for each RLC/EIS meter, thus measurements are not comparable. Therefore, the $\hat{Z}_G$ impedance must be minimized.

The DC sources are connected at the high-side of the standard. Each of the DC sources in the prototype is controlled by a D/A converter isolated at its digital side. The D/A converters generate the simulated cell voltage from 0 to 5 V. Simplified circuit diagram is shown in Fig. 3. Current path DC bias source is based on the power amplifier OPA548 which is capable to withstand full measurement current at 5V DC voltage. It must be cooled by a larger heatsink because it needs to dissipate peak power up to some 23 W. The floating supply is realized by a pair of DC/DC converters with asymmetric output voltages +9 V and -3.3 V. This range was chosen to minimize the power loss at the OPA548. The potential path DC bias source is based on operational amplifier OP211 and it is supplied from a low noise DC/DC converter with linear LDO regulators to reduce the noise. Both amplifiers are equipped by

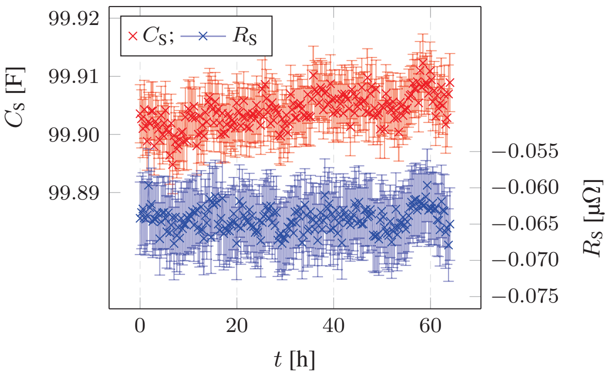

Fig. 6. Measurement of stability of 100 F impedance with rms current of 1 A and frequency 23 Hz. Note the uncertainty intervals were reduced to cover only stability of impedance bridge itself.

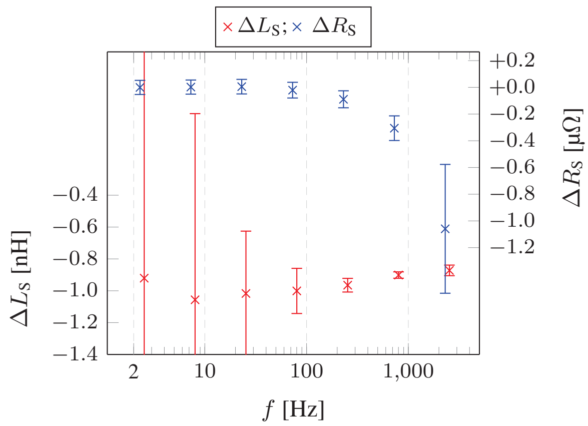

Fig. 7. Effective ground impedance between H_{POT} and L_{POT} terminals of simulated standard measured at 1 A.

stabilizing networks R_F, C_F and R_{OUT} to enable operation to large output capacitance C_{OUT} of 4x470 µF at their outputs realized by low-ESR polymer capacitors. The large capacitance ensures low source impedance at higher frequencies, whereas the feedback of amplifiers ensures low output impedance at low frequencies. Both sources are controllable either manually or via remote interface, so it is possible to perform automatic DC bias sweep measurement useful e.g. for testing EIS meter insensitivity to the applied DC bias voltage.

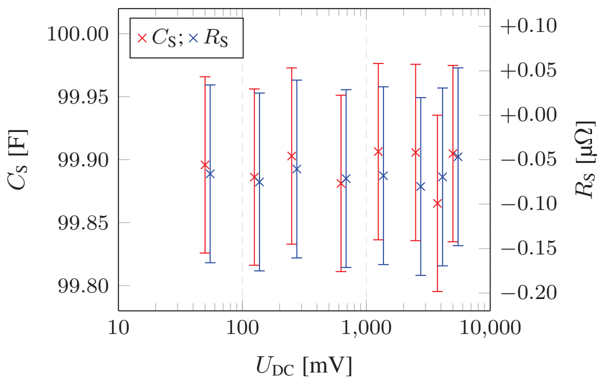

Fig. 8. Measurement of dependence of simulated impedance 100 F on the set DC bias at rms current 1 A and frequency 23 Hz. Note the uncertainty is limited by noise introduced by the DC bias source.

IV. MEASUREMENTS

A first prototype with mutual inductance of roughly 475 nH was constructed and characterized. Following measurements were performed by several methods. First, the impedance bridge [7] was used for measurements at higher frequencies without DC bias. Modified digital sampling wattmeter and a bridge [8] based on the digitizers NI 9238, NI 9239 and Keysight 3458A were used for the low frequency measurements and DC bias measurements.

Example of measured series capacitance for few selected frequencies is shown in Table. 1. As expected the value of impedance changes according to the equation 1 and except the highest frequencies it seems to match the calculated values. The observed series resistance is slightly negative which is expected because of the inverted polarity of the secondary winding. However, the loss tangent still stays at values not even remotely achievable by any physical standard of such capacitance, so this simple standard is almost pure reactance. Table. 1 also shows measurement of apparent inductance in noninverted secondary mode. As expected the series resistance in this case is inversion of the one measured in capacitive mode. The slight asymmetry is possibly caused by mutual couplings inside the standard. Just for curiosity the same measurement was repeated also in five-terminal (5T) definition. That is without considering the apparent shield impedance $\hat{Z}_G$ which is part of 4TP impedance definition. Es expected, the difference between 5T and 4TP measurements shown in Fig. 7 is reasonably small due to the strict internal separation of current and potential grounds and their joint in a single spot. However, it is not zero. Therefore, it is basically a calibration uncertainty limit in order to not risk different readings among particular RLC/EIS meters due to their imperfect 4TP measurement as explained above. However, 1 nH uncertainty of 475 nH value is still well within LiBforSecUse project goal of 1% uncertainty.

Graph in Fig. 8 shows dependence of simulated impedance on setting of its DC bias voltage. The observed dependence is affected by linearity of the digitizer as is discussed in [8]. This results to relatively high uncertainties, however no systematic change of impedance was observed in terms of the uncertainty.

Fig. 6 shows stability of simulated impedance measured over period of 60 hours. Value of capacitance changed

Table 1. Measured 4TP and 5T impedance of the prototype with approximate mutual inductance of 475 nH. Values are shown in series equivalent connection $C_S - R_S$ and for inductive mode (not inversed secondary) in $L_S - R_S$. Measurement was performed with rms current of 1 A. Uncertainties are expanded to $k = 2$.

a) Four terminal-pair (4TP)

f Hz	$\lvert Z \rvert$ mΩ	C_S F	R_S μΩ	D -	L_S nH	R_S μΩ
2305.5	6.884	0.010 027 61 ± 0.000 000 90	-8.70 ± 0.48	-0.001 26 ± 0.000 07	474.724 ± 0.033	7.58 ± 0.48
729.07	2.182	0.100 236 1 ± 0.000 004 2	-2.147 ± 0.092	-0.000 99 ± 0.000 04	475.023 ± 0.020	2.216 ± 0.092
230.55	0.691	1.001 767 ± 0.000 092	-0.468 ± 0.064	-0.000 68 ± 0.000 09	475.359 ± 0.043	0.512 ± 0.064
72.907	0.219	10.014 0 ± 0.002 8	-0.077 ± 0.059	-0.000 35 ± 0.000 27	475.53 ± 0.14	0.061 ± 0.059
23.055	0.069	100.133 ± 0.079	-0.036 ± 0.054	-0.000 52 ± 0.000 79	475.44 ± 0.39	0.014 ± 0.054
7.2907	0.022	1001.1 ± 2.5	-0.035 ± 0.053	-0.001 6 ± 0.002 4	475.5 ± 1.2	0.027 ± 0.053
2.3055	0.007	10007 ± 77	-0.023 ± 0.053	-0.003 3 ± 0.007 7	475.9 ± 3.7	0.030 ± 0.053

b) Five terminal (5T)

f Hz	$\lvert Z \rvert$ mΩ	C_S F	R_S μΩ	D -	L_S nH	R_S μΩ
2305.5	6.884	0.010 009 22 ± 0.000 000 90	-9.77 ± 0.48	-0.001 42 ± 0.000 07	473.852 ± 0.033	6.53 ± 0.48
729.07	2.182	0.100 045 4 ± 0.000 004 2	-2.451 ± 0.092	-0.001 13 ± 0.000 04	474.121 ± 0.020	1.909 ± 0.092
230.55	0.691	0.999 750 ± 0.000 092	-0.565 ± 0.064	-0.000 82 ± 0.000 09	474.394 ± 0.043	0.430 ± 0.064
72.907	0.219	9.992 9 ± 0.002 8	-0.100 ± 0.059	-0.000 46 ± 0.000 27	474.53 ± 0.14	0.043 ± 0.059
23.055	0.069	99.920 ± 0.079	-0.032 ± 0.054	-0.000 47 ± 0.000 79	474.42 ± 0.39	0.021 ± 0.054
7.2907	0.022	999.3 ± 2.5	-0.034 ± 0.053	-0.001 5 ± 0.002 4	474.4 ± 1.2	0.030 ± 0.053
2.3055	0.007	10004 ± 77	-0.024 ± 0.053	-0.003 5 ± 0.007 7	475.0 ± 3.7	0.029 ± 0.053

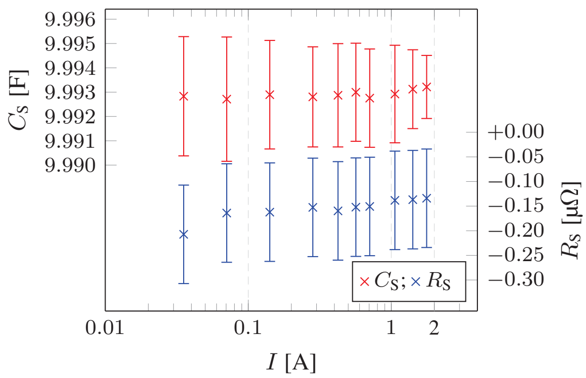

Fig. 9. Measurement of dependence of 10 F impedance on rms current level at frequency 73 Hz.

roughly by 0.005 % which is within possible instability of used digitizer. Resistance value stayed deep within the uncertainty. Fig. 9 shows dependence of 10 F impedance on rms AC current level. Resistance shows small dependence possibly due to self heating. No dependence outside uncertainty of measurement was found for capacitance which suggests no significant nonlinearity of the inductor.

V. CONCLUSION

An experimental capacitive reactance simulator based on the mutual inductor was designed. A prototype reaching apparent kilofarad capacitance at frequencies around 1 Hz was built and equipped by experimental DC bias sources that emulates lithium cell voltage. The standard was characterized for basic parameters and the results suggests it is usable for goals of the EMPIR project LiBforSecUse, where 1 % target uncertainty of impedances down to 1 mΩ is required. The standard exhibits loss tangent below 0.003 in most of the frequency range which is reasonably pure reactance. Effective shield impedance between H_{POT} and L_{POT} is around 1 nH, so the difference of the simulated capacitance between 5T and 4TP measurement definition is just around 0.2 %. That makes it suitable for comparable measurements among various RLC/EIS meters. The whole design was made open hardware so it is available for future development. Several problems were identified. The main problem is significant noise from the D/A converters used to set the simulated cell voltage. These should be replaced in the next prototype. Another problem is high common mode noise introduced from the isolating DC/DC converters and their large capacitive coupling. This may be solved by additional active guarding of the sources.

VI. ACKNOWLEDGMENT

Presented experimental standard was co-developed in scope of the EMPIR project LiBforSecUse (17IND10). The project received funding from the EMPIR programme co-financed by the Participating States and from the European Union's Horizon 2020 research and innovation programme.

REFERENCES

[1] MSU EURAMET. *European Metrology Programme for Innovation and Research (EMPIR)*. [online]. URL: http://msu.euramet.org/calls.html.

[2] MSU EURAMET. *EMPIR project - Lithium Batteries for Second Use*. [online]. URL: https://www.ptb.de/empir2018/libforsecuse/home/.

[3] F. Overney and B. Jeanneret. "Calibration of an LCR -Meter at Arbitrary Phase Angles Using a Fully Automated Impedance Simulator". In: *IEEE Transactions on Instrumentation and Measurement* 66.6 (June 2017), pp. 1516–1523. ISSN: 1557-9662. DOI: 10.1109/TIM.2017.2652500.

[4] M. Ouameur, F. Ziadé, and Y. L. Bihan. "Toward a Calculable Standard Shunt for Current Measurements at 10 A and Up To 1 MHz". In: *IEEE Transactions on Instrumentation and Measurement* 68.6 (June 2019), pp. 2215–2222. ISSN: 1557-9662. DOI: 10.1109/TIM.2018.2884553.

[5] B. P. Kibble. "Four terminal-pair to anything else!" In: *IEE Colloquium on Interconnections from DC to Microwaves (Ref. No. 1999/019)*. Feb. 1999, pp. 6/1–6/6. DOI: 10.1049/ic:19990102.

[6] Stanislav Mašláň. *EMPIR project Lithium Batteries for Second Use - Impedance simulator based on mutual inductor.* [online]. URL: https://www.GitHub.com/smaslan/Z-sim-mutual.

[7] Stanislav Mašláň et al. "Digital Sampling Setup for Measurement of Complex Voltage Ratio". In: *IEEE Transactions on Instrumentation and Measurement* 66.6 (June 2017), pp. 1355–1363. ISSN: 0018-9456. DOI: 10.1109/TIM.2017.2649899.

[8] Stanislav Mašláň. "Design of digital sampling impedance bridge for battery impedance spectroscopy". In: *Imeko 2020 TC4 International Symposium*. submitted 2020.